

## Diffraction Calculation of Arbitrarily Curved Wedge Modeled with NURBS Surfaces

Jun Yan<sup>1</sup>, Jun Hu<sup>\*, 1</sup>, Hua Peng Zhao<sup>2</sup>, and Zai Ping Nie<sup>1</sup>

**Abstract**—In this paper, we present an equivalent current-based numerical routine for calculating the diffraction of arbitrarily curved wedge modeled with non-uniform rational B-spline (NURBS) curves and surfaces. The NURBS curves and surfaces obtained from CAD systems need to be parameterized for numerical calculation; however, available parameterizing approaches in rendering computer graphics, which use straight line segments and flat facets for tessellation, are not suitable for the computation of the wedge diffraction. To make the full use of NURBS modeling technique in high-frequency asymptotic approaches, the proposed numerical routine utilizes a curvature adaptive tessellation scheme to parameterize the edge curve of the wedge with varying curvature as well as the method of parameter alignment to maintain the  $C^0$  continuity between the edge curve and the wedge surfaces, which is essential in evaluating the diffraction coefficients. Based on the proposed parameterizing method, the equivalent edge current can be implemented for diffraction computation of arbitrarily curved wedge modeled with NURBS curves and surfaces, complementing with the NURBS based physical optics (PO) as a fully NURBS-based high-frequency approach, which provides high geometrical accuracy and computational efficiency for calculating diffraction of electrically large curved wedges. Numerical examples are presented to validate the proposed method.

### 1. INTRODUCTION

It is often desirable to predict the scattering of the electrically large platform for RCS reduction design in electromagnetic (EM) engineering. Compared to full-wave analyzing tools such as the method of moment (MoM) or finite element method (FEM), the high-frequency asymptotic method can substantially reduce the requirement of computational resources, and it has continued to be a workhorse for electrically large problem solving.

The non-uniform rational B-spline (NURBS) modeling technique is able to provide accurate geometry description with less surface patches. Hence, NURBS modeling technique was introduced to high-frequency asymptotic approaches for practical purpose [1–3]. As the current-based method, the physical optics (PO) approximation is a favorable choice for scattering prediction owing to its ease of implementation and applicability to general cases. NURBS based PO (NURBS-PO) is therefore developed to predict the scattering of PEC bodies, where solving the critical points on the NURBS surface by the method of stationary point enables the NURBS-PO to enjoy a fast calculation of the PO integral on such parametric surface [1]. Further research on NURBS-PO adopts the equivalent current method of the physical theory of diffraction (PTD) framework to analyze the wedge diffraction, however, only the straight wedge case is considered [4]. To the authors's knowledge, the correction to curved wedge for NURBS-PO has not been reported yet.

---

*Received 6 July 2015, Accepted 7 August 2015, Scheduled 11 August 2015*

\* Corresponding author: Jun Hu (hujun@uestc.edu.cn).

<sup>1</sup> Department of Microwave Engineering, School of Electronic Engineering, University of Electronic Science and Technology of China, Chengdu 611731, P. R. China. <sup>2</sup> Department of Electronics and Photonics, A\*STAR Institute of High Performance Computing, Singapore.

Correcting the wedge discontinuity is consistent with previously developed NURBS-PO is challenging for several reasons. First, establishing the proper geometric description of a curved wedge in NURBS form is non-trivial. Most researches in literature use the straight wedge case as a trade-off between the geometric precision and computational efficiency. According to [5], the wedge could be defined by the intersection of two NURBS surfaces, however, despite the high complexity of solving the parameter surface intersecting, to compute the intersection for every surface-pair is unrealistic in real-life problem containing huge number of surfaces. Second, available parameterizing approaches developed to render the computer graphics for computer aided design (CAD) systems are not suitable for computing the equivalent edge currents, because only straight edges and flat facets can be obtained using those methods [6]. Moreover, the high-frequency approaches for calculating the scattered field are curvature sensitive to the geometry (which are sensitive to the curvature changing of the edge or surface), huge numbers of curves and patches could be obtained using these tessellation schemes. Furthermore, because the NURBS curves and surfaces are defined in their own parameter domains, calculating the equivalent edge current on the wedge is further hampered by maintaining the continuity  $C^0$  between the two surfaces and the edge curve that define the wedge structure. Existing parameter aligning technique developed in tracking the trace of creeping wave transition between parameter patches can overcome this difficulty. However, it requires a high computational cost and lacks flexibility for complicated cases [7].

In this paper, we present a numerical routine for calculating the diffraction of arbitrarily curved wedge modeled with NURBS curves and surfaces based on the equivalent current method (ECM). To make the proposed method fully NURBS based approach compatible to previously developed NURBS-PO, we adopt the geometry information from IGES standard file to define the arbitrarily curved wedge, as shown in Fig. 1, which is the fundamental geometry for further calculation. To parameterize the edge curve for evaluating the equivalent edge currents, the curvature adaptive scheme is developed to tessellate the edge curve with varying curvature. And then, on each tessellated curve segment, the method of parameter alignment is utilized to ensure the  $C^0$  parameter continuity between the edge curve and wedge surfaces. As a validation, we calculate the wedge diffraction by applying the Michaeli's equivalent edge current (EEC) [8] on the parameterized curved edge segments.

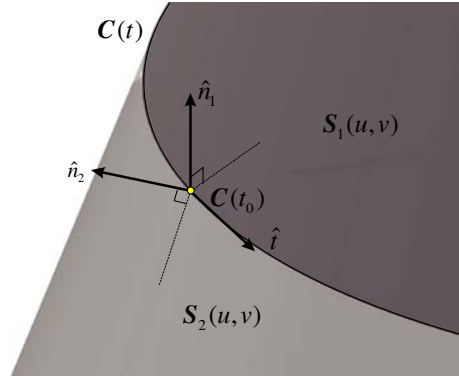


**Figure 1.** The geometry of a curved wedge defined by the NURBS curve  $\mathbf{C}(t)$  as well as two NURBS surfaces  $\mathbf{S}_1(u, v)$  and  $\mathbf{S}_2(u, v)$ .  $\mathbf{C}(t_0)$  is the edge curve point.  $\hat{t}$  is the unit tangential of  $\mathbf{C}(t)$  at  $t = t_0$ .  $\hat{n}_1$  is the unit normal of  $\mathbf{S}_1$  with respect to  $\mathbf{C}(t_0)$  and  $\hat{n}_2$  is the unit normal of  $\mathbf{S}_2$  with respect to  $\mathbf{C}(t_0)$ .

The rest of the paper is arranged as follows: detailed implementation of the proposed method is presented in Section 2; numerical results and discussions are given in Section 3; conclusions are drawn in the last section.

## 2. IMPLEMENTATION OF ECM ON THE NURBS MODELED CURVED WEDGE

The details of computing the diffraction of the curved wedge are presented in this section. The wedge curve is first tessellated in a curvature adaptive way. And then the EEC on each curve segment

is evaluated, where the surface-edge-surface  $C^0$  continuity is built up by the method of parameter alignment.

### 2.1. Conversions of Edge Curve and Wedge Surface

Numerical computations of normal and tangential are stable on the parameter curve and surface of rational Bezier form. Therefore, the NURBS curves and surfaces composing the wedge are initially converted to their corresponding rational Bezier forms using the Cox-de Boor algorithm [9]. The points on a rational Bezier curved are given by

$$\mathbf{C}(t) = \frac{\sum_{i=0}^m w_i B_i^m(t) \mathbf{P}_i}{\sum_{i=0}^m w_i B_i^m(t)} \quad t \in [0, 1] \quad (1)$$

where  $\mathbf{P}_i$  are the control points in  $\mathbf{R}^3$ ;  $w_i$  are the corresponding weights of  $\mathbf{P}_i$ ;  $m$  is the curve degree;  $B_k^s(t)$  is the Bernstein polynomial and defined as

$$B_k^s(t) = \frac{s!}{k!(s-k)!} t^k (1-t)^{s-k} \quad (2)$$

Meanwhile, the points on the rational Bezier patch are given by

$$\mathbf{S}(u, v) = \frac{\sum_{i=0}^m \sum_{j=0}^n w_{i,j} B_i^m(u) B_j^n(v) \mathbf{P}_{i,j}}{\sum_{i=0}^m \sum_{j=0}^n w_{i,j} B_i^m(u) B_j^n(v)} \quad \begin{matrix} u \in [0, 1] \\ v \in [0, 1] \end{matrix} \quad (3)$$

where  $\mathbf{P}_{i,j}$  are the control points of the surface in  $\mathbf{R}^3$ ,  $w_{i,j}$  are the weights of  $\mathbf{P}_{i,j}$ ,  $m$  and  $n$  are the surface degrees.

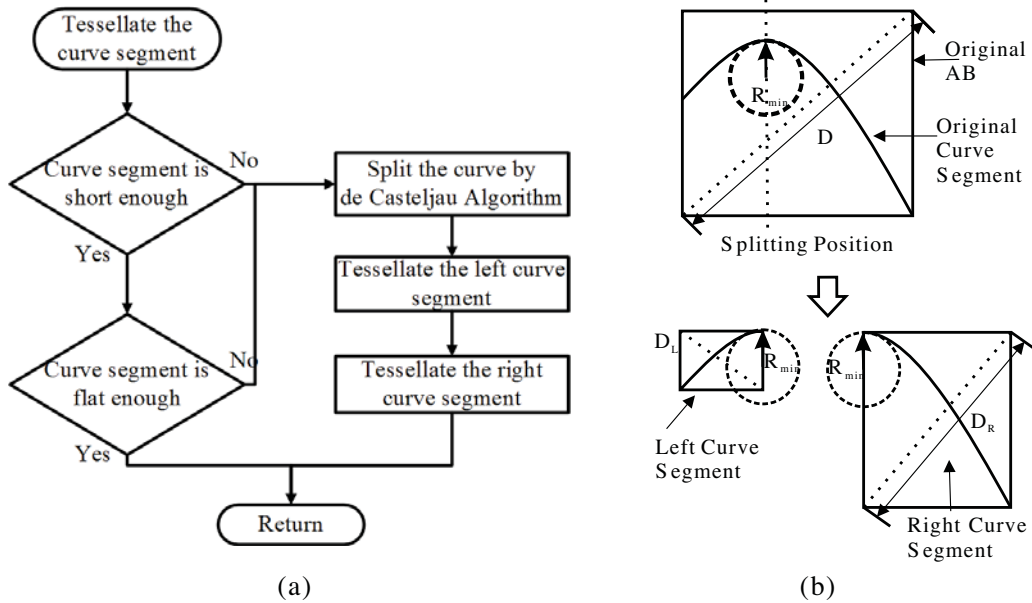


**Figure 2.** (a) The flowchart of the curvature adaptive tessellation algorithm; (b) the schematic of curvature based tessellation.

## 2.2. The Parametrization of Edge Curve

To ensure an accurate evaluation of EEC radiation integral on the edge with varying curvature, a curvature adaptive tessellation procedure is developed to refine the Bezier curve segments. Flowchart of the curvature adaptive tessellation procedure is presented in Fig. 2(a). The procedure utilizes de Casteljau algorithm for curve splitting to recursively tessellate a given curve segment [10]. Two termination conditions are employed to govern the tessellation. The first condition is to restrict the length of Bezier curve less than a given threshold. Because directly evaluating the Bezier curve length is computation-intensive in practice, the axis-aligned bounding-box (AB) technique is adopted as the substitution. According to the strong convex hull property of Bezier curve, the AB of a given Bezier curve can be constructed by finding the coordinate extremes of curve control points. Through the AB technique, the measure of curve length could be indicated by the diagonal of curve's AB. The second condition characterizes the flatness of Bezier curve, by which the curve can be tessellated in a curvature adaptive way. The flatness factor for a given curve segment is defined by

$$Flatness = \frac{D_{AB}}{R_{\min}} \quad (4)$$

where  $D_{AB}$  is the AB's diagonal length of the curve segment, and  $R_{\min}$  denotes the curve's minimum curvature radius, as shown in Fig. 2(b). It is noted that the tessellated Bezier curve segments using de Casteljau algorithm are geometrically equivalent to the original Bezier curves, which is the essence of keeping high geometrical accuracy for the proposed method. Moreover, compared with the approach that only uses the curve length as the tessellation governing condition [6], by defining the flatness of (4), the tessellation of the Bezier curve becomes curvature adaptive, which could reduce the number of the tessellated curve segments and thus improve the computational efficiency.

## 2.3. The Method of Parameter Alignment

In order to evaluate the EEC with respect to an edge curve point  $\mathbf{C}(t_0)$ , it is required to maintain a surface-edge-surface  $C^0$  continuity at  $\mathbf{C}(t_0)$ , which means to search for the corresponding parameter coordinates  $(u_1, v_1)$  and  $(u_2, v_2)$  on the wedge surfaces such that  $\mathbf{C}(t_0) = \mathbf{S}_1(u_1, v_1)$  and  $\mathbf{C}(t_0) = \mathbf{S}_2(u_2, v_2)$ . This is equivalent to the problem of solving the surface point  $\mathbf{S}(u, v)$  with a minimum distance to the given curve point  $\mathbf{C}(t_0)$ , where the curves and surfaces are given in their corresponding Bezier forms of (1) and (3). The distance vector function is written as

$$\mathbf{d}(u, v) = \mathbf{S}(u, v) - \mathbf{C}(t_0) \quad (5)$$

The distance between  $\mathbf{C}(t_0)$  and  $\mathbf{S}(u, v)$  is minimum if  $\mathbf{d}(u, v)$  is perpendicular to both surface tangential vectors in both  $u$ -direction and  $v$ -direction at  $\mathbf{S}(u, v)$ , which can be formulated as

$$F(u, v) = [F] = \begin{bmatrix} f(u, v) \\ g(u, v) \end{bmatrix} = \begin{bmatrix} \mathbf{d}(u, v) \cdot \mathbf{S}_u(u, v) \\ \mathbf{d}(u, v) \cdot \mathbf{S}_v(u, v) \end{bmatrix} = 0 \quad (6)$$

The problem of minimizing the distance between  $\mathbf{C}(t_0)$  and  $\mathbf{S}(u, v)$  now becomes solving the root of (6). The multi-dimensional Newton's iteration method is employed to solve the truncated Taylor's series of (6), which can be written in the following format

$$\begin{bmatrix} u_{n+1} \\ v_{n+1} \end{bmatrix} = \begin{bmatrix} u_n \\ v_n \end{bmatrix} + \begin{bmatrix} \Delta u \\ \Delta v \end{bmatrix} \quad (7)$$

where

$$\begin{bmatrix} \Delta u \\ \Delta v \end{bmatrix} = [J]^{-1} [F] \quad (8)$$

where the Jacobian matrix in (8) is given by

$$[J] = \begin{bmatrix} f_u & f_v \\ g_u & g_v \end{bmatrix} = \begin{bmatrix} |\mathbf{S}_u|^2 + \mathbf{d} \cdot \mathbf{S}_{uu} & \mathbf{S}_u \cdot \mathbf{S}_v + \mathbf{d} \cdot \mathbf{S}_{uv} \\ \mathbf{S}_u \cdot \mathbf{S}_v + \mathbf{d} \cdot \mathbf{S}_{vu} & |\mathbf{S}_v|^2 + \mathbf{d} \cdot \mathbf{S}_{vv} \end{bmatrix} \quad (9)$$

The combination of (6)–(9) can be considered as a parameter alignment technique for ensuring the surface-edge-surface  $C^0$  continuity. Generally, it is too time-consuming to maintain such continuity for the entire domain of each edge curve. For numerical implementation, the aforementioned parameter aligning procedure is only invoked at a finite number of samplings on the edge curve for EEC calculation.

### 2.4. Evaluation of the Diffracted Field on the Parameterized Curve Segments

The wedge diffracted field is evaluated by the radiation integral of equivalent edge current on the  $N$  segments of parameterized edge curve  $\mathbf{C}_i(t)$

$$\mathbf{E}_d^s(\mathbf{r}) = \sum_{i=1}^N \int_{\mathbf{C}_i} \mathbf{F}(\mathbf{r}') d\mathbf{r}' \tag{10}$$

where

$$\mathbf{F}(\mathbf{r}') = jk \frac{e^{-jk r}}{4\pi r} (Z_0 \hat{s} \times (\hat{s} \times \mathbf{I}(\mathbf{r}')) + \hat{s} \times \mathbf{M}(\mathbf{r}')) \tag{11}$$

$k$  is the wave number of the incidence,  $Z_0$  the wave impedance of free space, and  $\hat{s}$  the observation direction. In (11),  $\mathbf{I}(\mathbf{r}')$  and  $\mathbf{M}(\mathbf{r}')$  are equivalent edge currents whose calculation is detailed in [8].

### 3. RESULTS AND DISCUSSIONS

Examples are given to validate the proposed method. In all examples, the NURBS-based PO method in [10] is employed to evaluate the contribution of curved wedge surfaces.

In the first example, we study the backscattering from a standard PEC cylinder, as shown in Fig. 3(a), which is illuminated by the incident plane wave of 300 MHz from directions with  $\phi = 0^\circ$  and  $\theta$  ranging from  $0^\circ$  to  $180^\circ$ . Fig. 3(b) presents the results from MoM solver of commercial software FEKO, PO in [11] and the proposed method in this paper. As can be seen in Fig. 3, the proposed method in this paper agrees better with FEKO than the pure PO in [11], which demonstrates the effectiveness of the proposed method. As the second example, we investigate the capability of the proposed method in modeling curved wedge with a varying edge curvature, by evaluating the backscattering of the PEC elliptic cylinder under the plane wave illumination of 300 MHz, whose geometry is shown in Fig. 4(a). We compare the results of the proposed method with those of MoM at incident directions of  $\phi = 0^\circ$  and  $\theta$  ranging from  $0^\circ$  to  $90^\circ$  with an increment of  $\Delta\theta = 0.5^\circ$ . The mean relative error (MRE) is adopted to measure the level of agreement between the proposed method and MoM. Fig. 4(b) demonstrates the MRE under different combinations of curve length and the flatness. Table 1 lists the corresponding numbers of tessellated edge curve segments under different tessellation. According to Fig. 4(b) and Table 1, a reduction of MRE is observed with the decrease of diagonal length of AB. Under the same curve length condition, the MRE is also reduced as the flatness factor decreases. It is noticed that

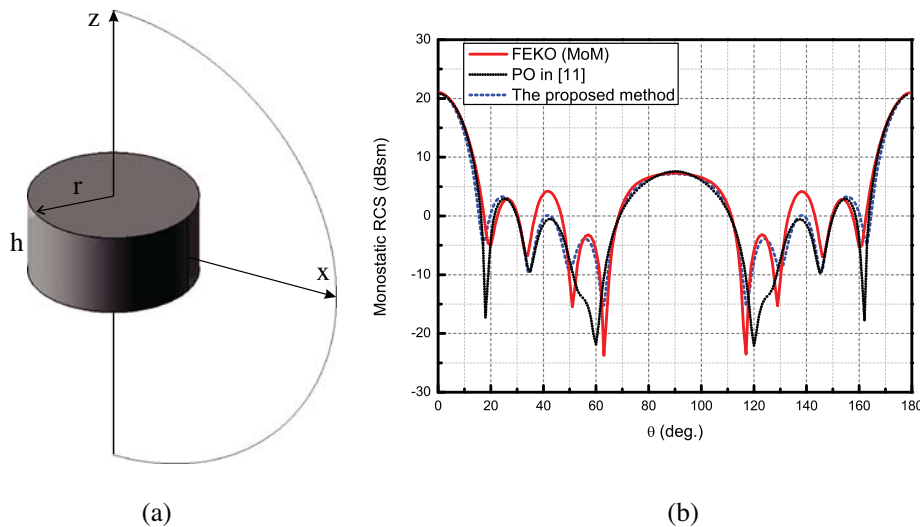


**Figure 3.** (a) Configuration of the PEC cylinder,  $r = 1.0m$  and  $h = 1.0m$ ; (b) backscattering of the PEC cylinder.

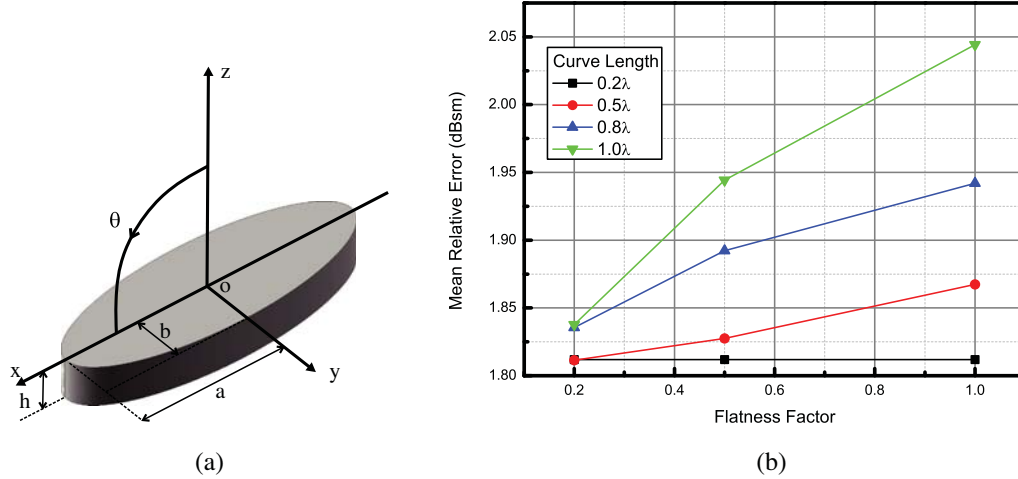


**Figure 4.** (a) Configuration of the PEC elliptic cylinder,  $a = 3.0m$ ,  $b = 0.5m$ ,  $h = 0.5m$ ; (b) mean relative error under different combinations of tessellating curve length and flatness.

**Table 1.** Statistics under different tessellation settings.

Curve Length ( $\lambda$ )	Flatness	Curve Segments	MRE (dB)
0.2	0.2	248	1.81
	0.5	224	1.81
	1.0	224	1.83
0.5	0.2	120	1.81
	0.5	88	1.81
	1.0	72	1.86
1.0	0.2	96	1.83
	0.5	64	1.94
	1.0	48	2.04

when the curve length drop to a relatively low level ( $0.2\lambda$  in this case), MRE is maintained at the same level, irrelevant to the change of flatness factor. However, when the curve length condition increases, the reduction of MRE becomes significant as the flatness decreases, indicating the effectiveness of the curvature adaptive tessellation scheme. It is also observed that, to achieve the same MRE level with small flatness factor, a relatively large curve length tessellation generates less number of curve segments than a small curve length tessellation. This is because the curvature adaptive tessellation terminates at the relatively flat curve segments while refining those curve segments with severe change of curvature.

In the last example, the backscattering of a mock PEC ship is investigated. The geometry of the ship is shown in both Fig. 5(a) and Fig. 5(b). It is illuminated by the plane wave of 300 MHz from directions of  $\phi = 0^\circ$  and  $\theta$  varying from  $0^\circ$  to  $180^\circ$ . Fig. 6 reports a comparison of results between the proposed method and the PO solver of FEKO. Table 2 lists the detailed statistics on CPU time of preprocessing and calculating as well as the patch number of both methods, where the item of preprocessing time includes the time consumption of importing the model and generating the mesh. As shown in Table 2, due to the parametric modeling technique adopted in the proposed method, the CPU time consumption of the proposed method is less than that of the triangular flat patch based FEKO under the same accuracy. The good agreement of results in Fig. 6 indicates that the presented method is capable of handling general problems in real-life.

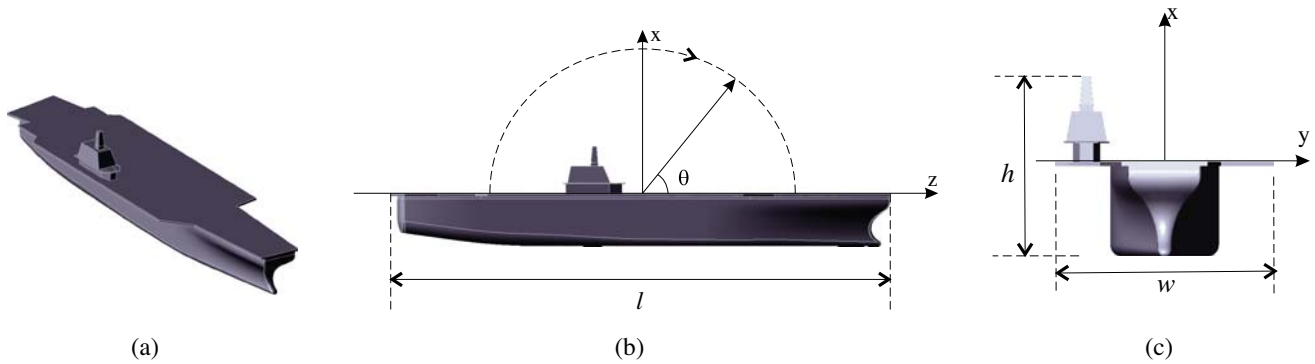


**Figure 5.** Configuration of the mock PEC ship, with 1,753 curved edge segments,  $l = 400.0m$ ,  $w = 97.0m$ ,  $h = 80.0m$ . (a) Perspective view; (b) side view; (c) front view.

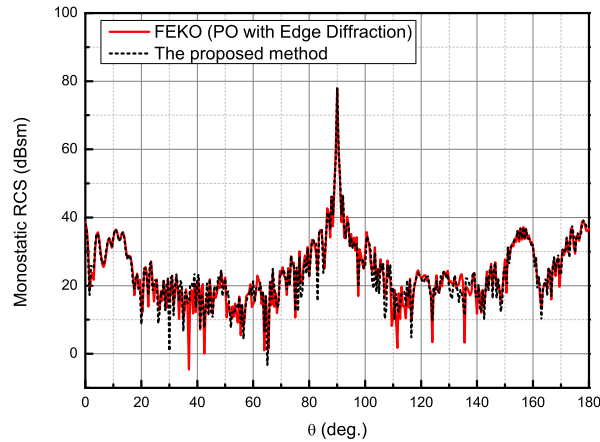


**Figure 6.** Backscattering of the PEC mock ship.

**Table 2.** CPU time consumption of the proposed method and FEKO for evaluating the RCS of the PEC ship(patch size is set as  $0.2\lambda$  for both the proposed method and FEKO).

Methods	Preprocessing Time(s)	Patch Number	Calculating Time(s)
FEKO	97	92,886	516
This paper	79	85,236	472

#### 4. CONCLUSIONS

In this paper, we present a numerical routine for calculating the diffraction of arbitrarily curved wedge modeled with NURBS curves and surfaces. Compared to traditional methods that use the straight wedge for computation, the proposed method retains geometrical accuracy of the model. The curvature adaptive edge parametrization enables the ECM to solve the diffraction of a curved wedge with changing curvature. The method of parameter alignment provides a general and robust numerical routine for maintaining the continuity between edge curve and wedge surfaces. Most importantly, the proposed method serves as a complementary to previously developed NURBS-PO methods and makes it possible to solve the electrically large problem using a fully NURBS modeling based high-frequency approach.

## ACKNOWLEDGMENT

This work is supported partly by the National Natural Science Foundation of China (No. 61271033), the Program of Introducing Talents of Discipline to Universities (No. b07046), and the National Excellent Youth Foundation (No. 61425010).

## REFERENCES

1. Perez, J. and M. F. Catedra, "Application of physical optics to the RCS computation of bodies modeled with NURBS surface," *IEEE Transactions on Antennas and Propagation*, Vol. 42, No. 10, 1404–1411, 1994.
2. Domingo, M., F. Rivas, J. Perez, R., P. Torres, and M. F. Catedra, "Computation of the RCS of complex bodies modeled using NURBS surfaces," *IEEE Antennas and Propagation Magazine*, Vol. 37, No. 6, 36–47, 1995.
3. Zhao, Y., X.-W. Shi, and L. Xu, "Modeling with NURBS surfaces used for the calculation of RCS," *Progress In Electromagnetics Research*, Vol. 78, 49–59, 2008.
4. De Adana F. S., I. G. Diego, O. G. Blanco, P. Lozano, and M. F. Catedra, "Method based on physical optics for the computation of the radar cross section including diffraction and double effects of metallic and absorbing bodies modeled with parametric surfaces," *IEEE Transactions on Antennas and Propagation*, Vol. 52, No. 12, 3295–3303, 2004.
5. Wang, N. X. J. Dang, H. B. Yuan, and C. H. Liang, "Study on curved wedge diffraction in NURBS-UTD method," *Microwave and Optical Technology Letters*, Vol. 55, No. 10, 2317–2321, 2013.
6. Balazs, A., M. Guthe, and R. Klein, "Efficient trimmed NURBS tessellation," *Journal of WSCG*, Vol. 12, No. 1–3, 2004.
7. Chen, X., S. Y. He, D. F. Yu, H. C. Yin, W. D. Hu, and G. Q. Zhu, "Geodesic computation on NURBS surfaces for UTD analysis," *IEEE Antennas and Wireless Propagation Letters*, Vol. 12, 194–197, 2013.
8. Michaeli A., "Equivalent edge currents for arbitrary aspects of observation," *IEEE Transactions on Antennas and Propagation*, Vol. 32, No. 3, 252–258, 1984.
9. Boehm, W., "Generating the Bezier points of B-spline curves and surfaces," *Computer Aided Design*, Vol. 13, No. 32, 356–366, 1981.
10. Farin, G., *Curves and surface for CAGD*, Morgan Kaufmann, San Francisco, 2004.
11. Yan J., J. Hu, and Z. P. Nie, "Calculation of the physical optics scattering by trimmed NURBS surfaces," *IEEE Antennas and Wireless Propagation Letters*, Vol. 13, 1640–1643, 2014.